The hysteresis loops of magnetic ferrites and the processes involved in their formation

LYNN J. BRADY
Box 300, Route 2, Camden, South Carolina 29020, USA

It is shown that a specimen's microstructure affects the form of its magnetization curves but not M_s, the saturation magnetic moment per cm^3 nor H_s, the applied field strength required for saturation. A procedure is then given for the precise determination of M_s and H_s using data derived from the hysteresis loops of polycrystalline isotropic specimens. The procedure is simple to use and avoids the laborious extrapolation requirements of the "law of approach". Finally, the magnetization processes involved in forming the hysteresis loops between H_s and $-H_s$ are described.

1. Introduction

Bozorth claims [1] that adequate theory is not available to permit magnetization curves to be calculated at field values less than those corresponding to residual induction. This claim is supported by the inability of well-known models such as that of Stoner and Wohlfarth [2] to account for the magnetization of specimens in the second and fourth quadrants.

This paper provides the theory for these calculations. To support this theory, the magnetization of an arbitrary specimen is followed precisely between H^A, the positive anisotropy field value ([3] p. 47) and $-H^A$.

2. Fundamental concepts

The provided theory is based on the discovery that only two processes are involved in magnetizing or demagnetizing a specimen composed of perfect single-domain crystallites in a glass matrix [4]. These follow each other in succession when the strength of H_a, the applied field is changed sufficiently. In the first process, macrodomains are created irreversibly from the specimen's microdomains as H_a is increased in value. After all microdomains are consumed the magnetization vector of each macrodomain rotates reversibly in the applied field direction. This process continues as the strength of H_a is increased without limit

when the configurational entropy of each macrodomain equals zero and its volume remains constant. Under these conditions the magnetization vectors cannot turn over. These conclusions are based on thermodynamics [4] supported by data extending from $H_a = 0$ to 35 000 Oe.*

Use of the terms micro- and macrodomains follows precedent [4]. Thus, a microdomain exists only within its host crystallite. A macrodomain, however, is formed at a critical applied field value at which the walls of a number of adjoining microdomains snap [5]. Each of these microdomains has a size corresponding to that of its host crystallite. It is evident, therefore, that the macrodomain formed contains a number of crystallites within its boundaries.

Three magnetization processes follow each other in succession as the field applied to a specimen comprised of imperfect single-domain crystallites is increased in strength until it equals H^A. First, macrodomains are created irreversibly from the specimen's microdomains at low field values. After all microdomains are consumed, the macrodomains' magnetization vectors rotate reversibly in the applied field direction as H_a is increased in value. This rotation is accompanied by the irreversible turnover of all vectors pointing in the reverse field direction. This occurs according to thermodynamics [4] because the configur-

---

* Measurements made as a courtesy of Professor A. E. Miller of Notre Dame University who used a vibrating sample magnetometer.

ational entropy of the specimen's constituent crystallites does not equal zero.

Vector turnover becomes complete when the applied field strength equals H_s. Then between H_s and H^A the magnetization vectors rotate reversibly as H_a is changed in value. In addition, the macrodomains with the most favourable orientations grow reversibly at the expense of their less favourably oriented neighbours.

3. The initial demagnetization process

The virgin magnetization curves of the specimens referred to are reproduced in Fig. 1 for convenience. These specimens were prepared [4] by water quenching melts comprised of a complex barium
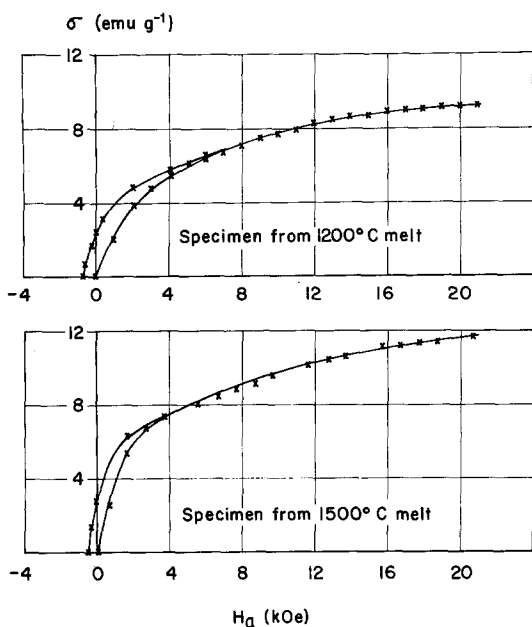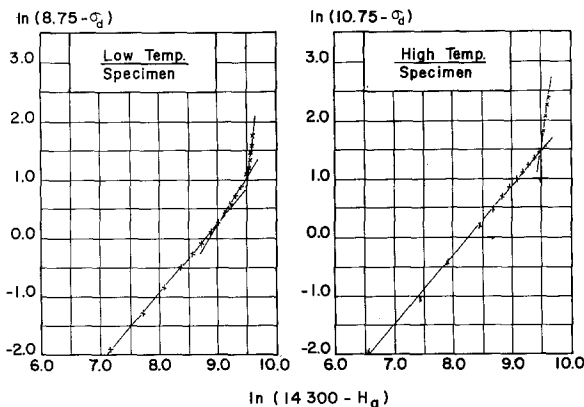

Figure 1 The virgin magnetization curves of specimens produced from 1200 and 1500° C melts.

ferrite ([3] p. 177) and glass. The specimen produced by the 1200° C melt contained imperfect crystallites. However, the crystallites formed on pouring the 1500° C melt were perfect. These conclusions are based on SEM micrographs and the characteristics of the specimens' ln–ln plots of H_a versus σ_n [4]. Here, σ_n is the normal magnetic moment per gram.

A break is observed at $H_s = 14\,300$ Oe in the 1200° C specimen's ln–ln plot of H_a versus σ_d. The term σ_d, introduced here is the magnetic moment per gram observed when the specimen is demagnetized. This break leads to the conclusion that reversible growth of macrodomains cannot take place when H_a is less than H_s. Consequently, a ln–ln plot of $(14\,300 - H_a)$ versus $(8.75 - \sigma_d)$ was prepared in order to determine the processes which take place in the 1200° C specimen as H_a is reduced from H_s. The plot prepared by means of data from Fig. 1 is shown in Fig. 2. This figure also shows the ln–ln plot of $(14\,300 - H_a)$ versus $(10.75 - \sigma_d)$ for the high-temperature specimen. The terms 8.75 and 10.75 in this figure are the magnetic moments per gram of the specimens in the field, $H_a = 14\,300$ Oe.

The ln–ln plot for the high-temperature specimen shows that between $H_a = 14\,300$ and 1600 Oe its magnetization vectors rotate reversibly in the reverse field direction. Then between $H_a = 1600$ Oe and H_{ci}, the intrinsic coercive force field, irreversible collapse of macrodomains occurs thereby partially reforming the specimen's microdomain structure.

By analogy it is concluded that the low-temperature specimen's magnetization vectors rotate reversibly in the reverse field direction as H_a is reduced from 14 300 to 5800 Oe. Then it is

Figure 2 Ln–ln plots of $(14\,360 - H_a)$ versus $(8.75 - \sigma_d)$ and $(14\,360 - H_a)$ versus $(10.75 - \sigma_d)$ for the specimens produced from the melts.
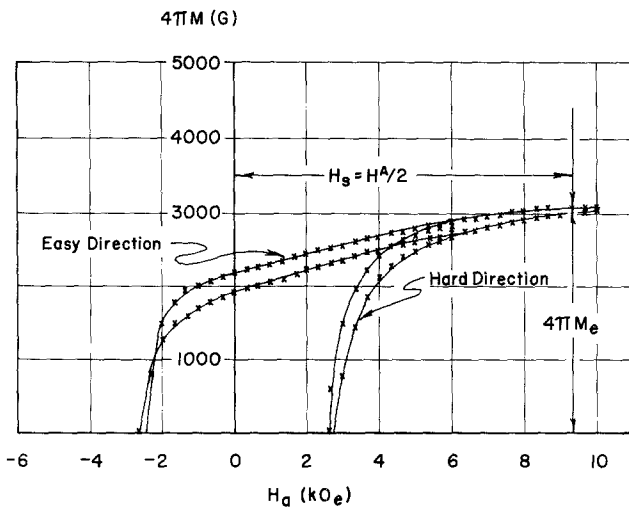
Figure 3 Hysteresis loops of a cubic $SrFe_{12}O_{19}$ specimen fired to obtain a product with a high coercive force.

assumed that between 5800 and 550 Oe spike and closure domains are formed. This irreversible process reduces the internal energy of the specimen to the minimum value it can have without micro-domain formation when its temperature and pressure are held constant. Again by analogy it is concluded that between 550 Oe and H_{ci} a portion of the specimen's macrodomains collapse irreversibly. This partially reforms the original microdomain structure.

4. The determination of H_s and M_s for a specimen comprised of polydomain crystallites

A ln–ln plot of $(H_s - H_a)$ versus $(4\pi\bar{M}_s - 4\pi\bar{M})$ is used to distinguish the magnetization process which take place between H_s and $-H_s$ in a specimen comprised of polydomain crystallites. The term $4\pi\bar{M}_s$, introduced here, is the saturation induction of a synthetic isotropic specimen and

$4\pi\bar{M}$ is its induction in the field H_a. The value of $4\pi\bar{M}$ is derived from the hysteresis loops of an arbitrary real specimen. This is done by averaging its inductions in the hard and easy directions of magnetization at the selected field value. This procedure makes it evident that the real specimen need not be isotropic.

The values of H_s, $4\pi\bar{M}_s$ and $4\pi\bar{M}$ of two cubic $SrFe_{12}O_{19}$ specimens are determined by means of the hysteresis loops shown in Figs. 3 and 4. The specimen whose hysteresis loops appear in Fig. 3 was fired to obtain a product with a high coercive force. The other specimen, however, was grossly overfired to induce excessive grain growth. As a result the specimen's hysteresis loops shear as shown. This procedure was followed to see if grain growth effects the specimen's H_s and M_s values.

The hysteresis loops in Figs. 3 and 4 are those of the specimens at $20°C$ obtained by means of a Magnemetrics Hysteresisgraph with pole coils.
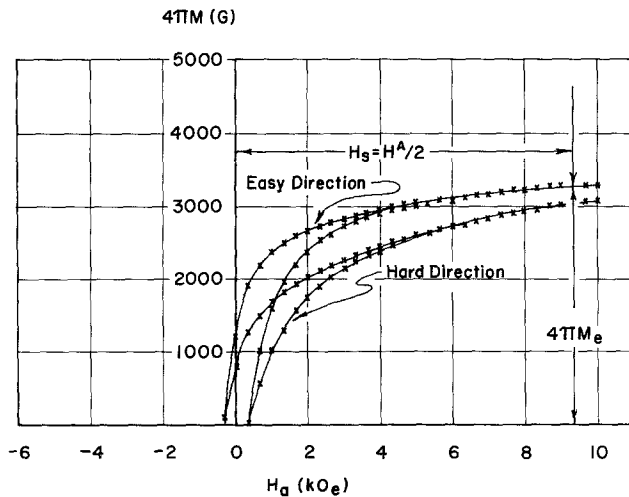

Figure 4 Hysteresis loops of a grossly over-fired cubic $SrFe_{12}O_{19}$ specimen.
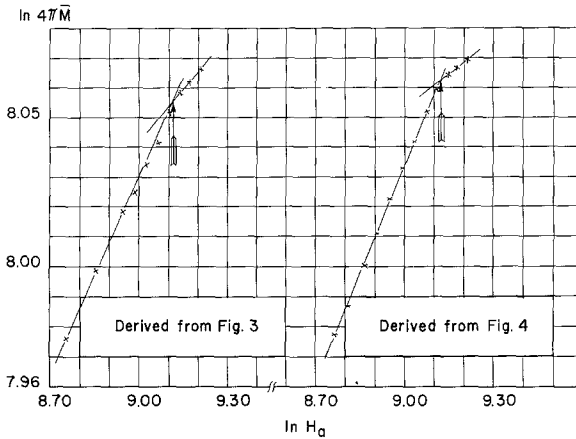
479

Figure 5 Ln–ln plots of H_a versus $4\pi\bar{M}$ for the ferrite specimens.

Those for the easy directions of magnetization were obtained by applying the fields to the respective specimens in the direction used to compact the calcine from which they were made. The curves for the hard direction, on the other hand, were obtained by applying the fields normal to the direction of compaction. The term, $4\pi\bar{M}_e$, in these figures, is the induction at H_s for the easy direction of magnetization and the relation, $H_s = H^A/2$ applies [6] because $SrFe_{12}O_{19}$ crystals are uniaxial in form.

Data from Figs. 3 and 4 were used to construct the ln–ln plots of H_a versus $4\pi\bar{M}$ shown in Fig. 5. Each plot in this figure has two segments which intersect at the points, $(\ln H_s, \ln 4\pi\bar{M}_s)$, indicated by the arrows. These points of intersection yield the value 9135 Oe for H_s. Since a field of this strength is required to saturate each specimen at 20° C, it is evident that grain growth does not change the value of H_s.

Fig. 5 also yields the values $4\pi\bar{M}_s = 3155$ and 3175 G. The specimen with the saturation induction of 3155 G had a density of $4.87 \, \text{g cm}^{-3}$ at 20° C and contained 2.80% impurities by weight. The other specimen with the sheared hysteresis loops had a density of $4.90 \, \text{g cm}^{-3}$ at 20° C. It contained 2.50% impurities by weight [6]. These density values are appreciably less than $5.11 \, \text{g}$ cm^{-3} reported [7] to be the X-ray density of $SrFe_{12}O_{19}$ at 20° C.

By means of these quantities, the term $\bar{D}/2N = 9/4\pi$ for a cubic specimen [6] and the equation,

$$4\pi\bar{M}_s = 4\pi M_s f\bar{D}/2N, \qquad (1)$$

the duplicate values, $M_s = 378$ and $377 \, \text{G cm}^{-3}$ are derived for $SrFe_{12}O_{19}$ at 20° C. These values are without doubt more precise than $M_s = 380 \, \text{G}$ cm^{-3} derived [7] by means of a single-crystal

specimen of $SrFe_{12}O_{19}$ at 20° C using empirical extrapolation procedures [8]. Moreover, they show that grain growth does not effect the value of M_s.

The term f, in Equation 1, is the normalization factor which takes into account the purity of the specimen and its relative density. $\bar{D}$ is the demagnetization factor of shape anisotropy for the constituent crystallites of a synthetic isotropic specimen and N is the real specimen's self-demagnetization coefficient.

5. The magnetization processes in a specimen comprised of polydomain crystallites

The magnetization processes which take place in the specimen whose hysteresis loops appear in Fig. 4 are established by means of the ln–ln plots of $(9135 - H_a)$ versus $(3155 - 4\pi\bar{M})$ shown in Figs. 6 and 7. These plots derived from Fig. 4 cover the ranges, H_s to H_{ic} and $-H_{ic}$ to H_s.

Analogy leads to the conclusion that demagnetization of the specimen between 9135 and 4905 Oe is associated with the reversible rotation of its magnetization vectors in the reverse field direction. Reducing H_a from 4905 to -860 Oe produces spike and closure domains. Since this is an irreversible process minor hysteresis loops are formed under the proper conditions between $H_a = 4905$ Oe and $-H_s$. Between -860 and -1915 Oe all macrodomains collapse irreversibly forming microdomains in the process. The microdomains formed have volumes corresponding to those of the specimen's constituent crystallites.

Fig. 7 is now used to establish the magnetization processes which take place in the specimen as the applied field is reduced in strength still further. It shows that the third and fourth segments of
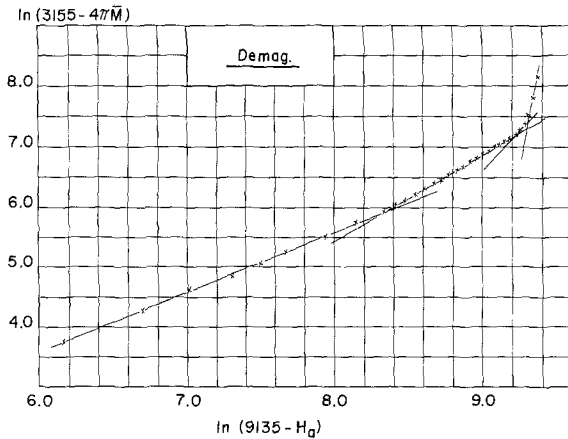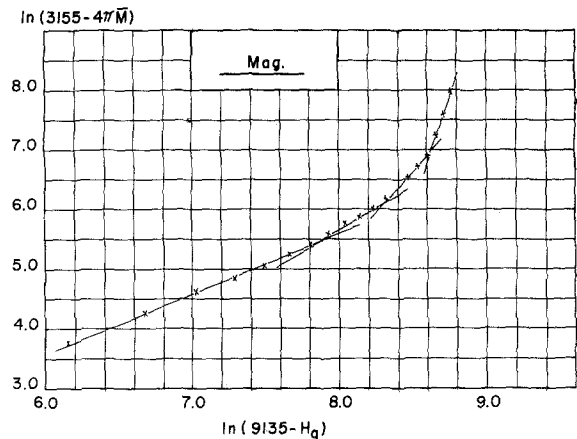
480

Figure 6 Ln–ln plots of $(9135 - H_a)$ versus $(3155 - 4\pi\bar{M})$ derived from the demagnetization curves in Fig. 3.

Figure 7 Ln–ln plots of $(9135 - H_a)$ versus $(3155 - 4\pi\bar{M})$ derived from the magnetization curves in Fig. 3.

the ln–ln plot intersect at the point where $H_a = 3510$ Oe. It is concluded, therefore, on the basis of symmetry that between -1915 and -3510 Oe the volumes of the microdomains decrease reversibly and in the process produce additional micro-domains. This process reduces the internal energy of the specimen to the minimum value it can have at $20°$C. Consequently, increasing H_a from -3510 Oe until it equals zero demagnetizes the specimen completely.

However, if H_a is reduced from -3510 to -5030 Oe microdomains with favourable orientations in the negative field direction grow reversibly at the expense of their less favourably oriented neighbours. At $H_a = -5030$ Oe, the volumes of the microdomains again correspond to those of the specimen's constituent crystallites.

Further reduction to the applied field strength leads to the irreversible formation of macrodomains at the expense of the specimen's microdomains. All microdomains are consumed by this process between -5030 and -6490 Oe. Then between -6490 Oe and $-H_s$, irreversible turnover of the

specimen's magnetization vectors pointing in the positive field direction takes place. In this field range reversible rotation of vectors not actually turning over also occurs.

Ln–ln plots of $(9135 - H_a)$ versus $(3175 - 4\pi\bar{M})$ for the specimen whose hysteresis loops shear drastically show that grain growth does not effect the sequence of the magnetization processes between H_s and $-H_s$. They do show, however, that the applied field values where the magnetization processes change are altered greatly by grain growth.

6. Conclusions

The magnetization processes which take place between H^A and $-H^A$ have been described. This description, however, failed to mention the magnetization associated with the specimen's domains of reverse magnetization. Neglecting this process is justified on the grounds that this caused no discernible error and an earlier report [4] discussed it thoroughly.

The simple procedure we introduced for the

481

determination of H_s and M_s is based on thermodynamics [4]. Since it avoids the laborious, empirical extrapolation procedure required by the "law of approach" [8] it should be welcomed.

References

1. RICHARD M. BOZORTH, "Ferromagnetism" (Van Nostrand, New York, 1953) p. 582.
2. E. C. STONER and E. P. WOHLFARTH, *Phil. Trans. Roy. Soc. London* **240A** (1948) 599.
3. J. SMIT and H. P. J. WIJN, in "Ferrites" (Wiley, New York, 1959).
4. LYNN J. BRADY, *J. Mater. Sci.* **12** (1977) 2115.
5. R. W. DeBLOIS, as cited by G. D. Cullity, "Introduction to Magnetic Materials" (Addison-Wesley, Reading, 1972) p. 308.
6. LYNN J. BRADY, *J. Mater. Sci.* **10** (1975) 697.
7. B. T. SHIRK and W. R. BUESSEM, *J. Appl. Phys.* **40** (1969) 1294.
8. K. H. STEWART, "Ferromagnetic Domains" (Cambridge University Press, 1954) p. 34.